Superlattices and Microstructures 113 (2018) 678–683

Contents lists available at ScienceDirect

Superlattices and Microstructures

journal homepage: www.elsevier.com/locate/superlattices

Leakage current transport mechanism under reverse bias in Au/Ni/GaN Schottky barrier diode

Koteswara Rao Peta [a, *], Moon Deock Kim [b]

[a] Department of Electronic Science, University of Delhi South Campus, Benito Juarez Road, New Delhi, 110021, India
[b] Department of Physics, Chungnam National University, 220 Gung-dong, Yuseong-gu, Daejeon, 305-765, Republic of Korea

ARTICLE INFO

Article history:
Available online 27 November 2017

Keywords:
GaN
Schottky barrier diode
Leakage current
Variable-range hopping
Poole-Frenkel emission

ABSTRACT

The leakage current transport mechanism under reverse bias of Au/Ni/GaN Schottky diode is studied using temperature dependent current-voltage (I-V-T) and capacitance-voltage (C-V) characteristics. I-V measurement in this study is in the range of 140 K–420 K in steps of 10 K. A reduction in voltage dependent barrier height and a strong internal electric field in depletion region under reverse bias suggested electric field enhanced thermionic emission in carrier transport via defect states in Au/Ni/GaN SBD. A detailed analysis of reverse leakage current revealed two different predominant transport mechanisms namely variable-range hopping (VRH) and Poole-Frenkel (PF) emission conduction at low (<260 K) and high (>260 K) temperatures respectively. The estimated thermal activation energies (0.20–0.39 eV) from Arrhenius plot indicates a trap assisted tunneling of thermally activated electrons from a deep trap state into a continuum of states associated with each conductive threading dislocation.

1. Introduction

The wide band gap (3.4 eV at room temperature), high electrical break down field and tunable band gap of gallium nitride (GaN) alloyed with aluminum and indium [1], made GaN a promising material for AlGaN/GaN high electron mobility transistors (HEMTs), power rectifiers, light emitting diodes (LEDs), and field-effect transistors (FETs) [2–5]. However, reverse leakage current in GaN is critical for making reliable electronic devices, since carrier trapping in defects degrades the lifetime and high power/high frequency operation. High concentration threading edge/screw type dislocations [6] and deep level defects in GaN film are the main sources of leakage current at room temperature, which are added to semiconductor materials at growth time or lack of sui⧹le substrate. Several methods have already been proposed such as chemical treatments [7], annealing processes [8] to suppress the influence of these defects on reverse leakage current in GaN. But the exact physical mechanism of reverse leakage transport in GaN based devices is not yet well understood.

The metal/semiconductor rectifier is a fundamental device for investigation on reverse leakage mechanism in semiconductor materials, which are used in modern electronic industry. Different kinds of transport mechanisms have already been reported for the leakage current in GaN at reverse bias [9–14]. For instance, Miller et al. suggested two kinds of transport mechanisms for reverse leakage current in Schottky barrier diode (SBDs) fabricated with GaN grown by molecular-beam epitaxy. They are field emission tunneling and trap assisted tunneling below and above 275 K temperature respectively

* Corresponding author.
E-mail address: krao@south.du.ac.in (K.R. Peta).

https://doi.org/10.1016/j.spmi.2017.11.056
0749-6036/

[10]. Zhang et al. described that the leakage current is dominated by tunneling below 150 K whereas the Poole-Frenkel emission (PFE) is a dominating mechanism at higher temperatures for both GaN and AlGaN/GaN SBDs [12]. Rao et al. explained the reverse leakage current mechanism in Ga-polarity GaN film grown by molecular beam epitaxy (MBE) on Si substrate using PFE model [13]. However, the reverse leakage current transport mechanisms in SBDs made with GaN grown by metal organic chemical vapor deposition (MOCVD) are not yet fully understood.

In this work we are reporting transport mechanisms of the reverse leakage current in GaN film grown by MOCVD with Ni/Au Schottky contact using temperature-dependent reverse bias current-voltage (I-V) characteristics and capacitance–voltage (C–V) characteristics measured at room temperature.

2. Experimental details

In this work, we used 3.5 μm thick GaN film grown at 1130 °C on sapphire (Al_2O_3) with 30 nm thick GaN grown at 550 °C as a buffer layer using MOCVD. The schematic structured layers of GaN grown on sapphire can be seen in Fig. 1 (a). The estimated unintentionally doped concentration and sheet resistivity (R_s) by Hall-effect measurements are ~1.2×10^{16} cm^{-3} and ~802 Ω/□ respectively. The SBD structure consists of square shaped Schottky Ni/Au (30 nm/200 nm) contact of an area 390×390 μm^2 surrounded by Ohmic [Ti/Al/Ni/Au (30 nm/40 nm/40 nm/200 nm)] contact. Electron beam evaporation system was used to make metal contacts. Rapid thermal annealing is conducted before Schottky contact formation on Ohmic contact at 800 °C for 30 s in nitrogen ambient. The reverse bias I-V characteristics as a function of temperature for GaN SBD were measured using Keithley measure unit (Model No.236) in steps of 10 K from 140 K to 420 K. Liquid nitrogen (LN_2) cryostat is used for low temperature characterization. C–V measurements at room temperature were performed at a fixed frequency of 1 MHz using Boonton capacitance meter (Model No. 7200).

3. Results and discussion

For rectifiers, the C-V measurement is one of the most powerful non-destructive methods for obtaining information about junction region. The room temperature experimental C-V characteristics were measured at frequency of 1 MHz as given in inset Fig. 1(b) as C^{-2} versus V plot, this plot can be used for calculation of carrier concentration and barrier height using the relation given [15,16]

$$\frac{d(C^{-2})}{dV} = \frac{2}{q\varepsilon_s A^2 N_d} \tag{1}$$

where ε_s is the permittivity of GaN ($\varepsilon_s = 9.5\varepsilon_0$), N_d is carrier concentration and A is area of Schottky contact. Further the barrier height is given as

$$q\varphi_B = qV_{bi} + qV_n \tag{2}$$

where $V_n = (kT/q)\ln(N_c/N_d)$ is the depth of Fermi level below conduction band. N_d is the effective density of states in conduction band, N_c is given by the relation $N_c = 2(2\pi m^* k_B T/h^2)^{3/2}$, where, $m = 0.22m_o$ with value 2.38×10^{18} cm^{-3} [17] for GaN at room temperature. Built-in voltage $V_{bi} = 1.09$ V is obtained from linear fit intercept on voltage axis of the data rage from 0 V

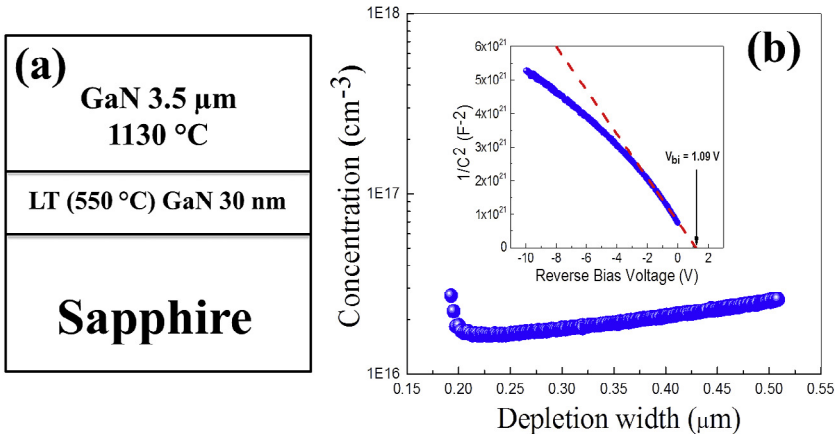

Fig. 1. **(a)** Schematic view of GaN thin film grown on sapphire substrate by MOCVD used in this study. **(b)** The distribution of carrier concentration in the depletion region, obtained from reverse bias C-V characteristics for Au/Ni/GaN SBD measure at room temperature in the voltage range 0–10 V and the built-in voltage $V_{bi} = 1.09$ V is obtained from $1/C^2$ versus V plot (inset Fig. 1(b)).

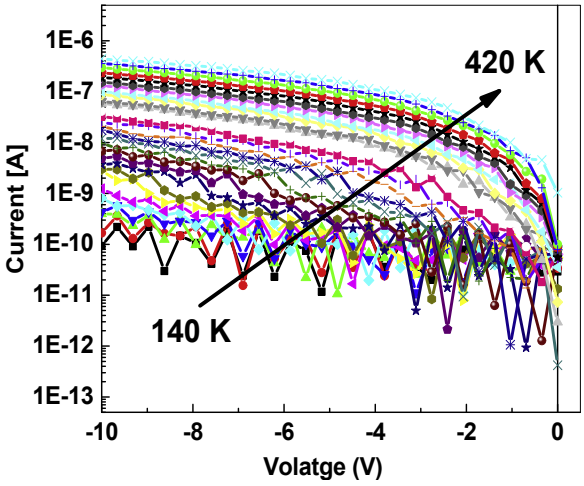

Fig. 2. Reverse bias Current-voltage characteristics of Au/Ni/GaN Schottkt barrier diode measured in the temperature rage 140 K–420 K in step of 10 K.

to 3.75 V [inset Fig. 1 (b)]. The estimated barrier height from C-V characteristics is 1.12 eV. The Fig. 1(b) is a plot of carrier concentration as a function of depletion width, the carrier concentration was found to increase with increase in depletion width. The increase in carrier concentration is due addition of donor type deep level defects as the depletion region penetrates more into GaN [18]. The donor type impurities in GaN are due to Nitrogen vacancies in GaN. The small depletion width indicates a very strong internal electric field in the space charge region.

Fig. 2 shows the experimental reverse bias I-V characteristics in semi-logarithmic scale for Au/Ni/GaN SBD in the temperature ranging from 140 K to 420 K in steps of 10 K. Clearly it is observed that, non-saturating current under reverse bias and dependence of current on both electric field and temperature. Generally reverse leakage current in metal/semiconductor SBD is due to thermionic emission over the barrier, which is small and negligible [19], which normally is attributing to saturation of reverse bias current

$$I(T) = AA^{*}T^{2}\exp\left(\frac{-q\varphi_{bo}}{kT}\right) \tag{3}$$

where A is the junction area, A^{*} is the effective Richardson contact (26.4 $Am^{-2}K^{-2}$ for GaN), k is the Boltzmann's constant and q is the charge of electron. Hence, the excess reverse leakage current, particularly in GaN like wide band gap semiconductor is not by the thermionic emission. But, current under reverse bias for Au/Ni/GaN SBD is showing non-saturating behavior with reduction of barrier height (BH) with increasing reverse bias voltage is shown Fig. 3.

Recently, Tomer et al reported similar kind of barrier heights as a function of bias voltage for Graphene based schottky contacts to various semiconductors (Si-Sic, C-SiC, GaAs and Si) [20].

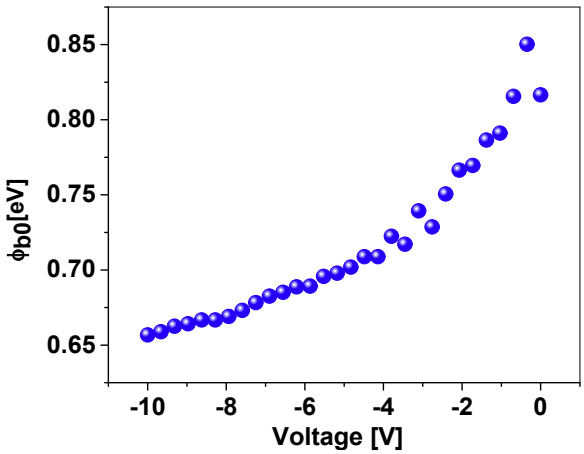

Fig. 3. Voltage dependent barrier height for Au/Ni/GaN SBD obtained from I-V characteristics measured at 300 K.

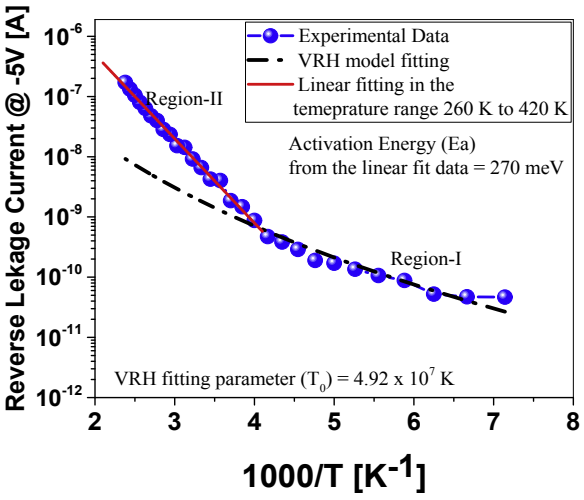

Fig. 4. Typical Arrhenius plot of reverse leakage currents measured at − 5 V of Au/Ni/GaN SBD. A VRH conduction model is fitted in the temperature range 140–250 K. Thermal activation energy estimated from data in the temperature range 260–420 K.

In order to explain mechanisms involved in the excess leakage current under reverse bias in account of reduction of barrier height with increasing voltage we have applied the variable-range-hopping (VRH) and Poole-Frenkel (PF) emission models. VRH conduction explains the charge carriers hopping conduction from one deep center to another deep center and the PF emission refers to electric-field-enhanced thermal emission from a trap state into a continuum of electronic states [14]. Fig. 4, reverse leakage current at −5 V versus inverse of temperature so called Arrhenius plot reveals that, two distinct reverse leakage current mechanisms were associated within wide temperature range of 140–420 K, Region-I. In the low temperature range (140–260 K) the reverse leakage current was found to be following the Mott's $T^{-\frac{1}{4}}$ law $\left(I\alpha\left\{\left(-\frac{T_0}{T}\right)^{1/4}\right\}\right)$ well fitted with a characteristic temperature of 4.92×10^7 K, which is a reasonable value falling within the typical range 10^6–10^9 K [21] and is good in agreement with the reported value 4.4×10^7 K for the GaN ($N_D \approx 9.7 \times 10^{16} cm^{-3}$) [22]. However, Mott's law does not fit the data well where the leakage current exponentially increases with decrease of 1/T, Region-II (>260 K). The possible physical mechanism associated with this thermally activated current component is a two-step, trap assisted tunneling process [10]. Similar kind of behavior has been observed by Jeong et al for GaInN LED and n-ZnO:Al/p-GaN:Mg hetero-junction LED respectively [23]. A linear fit of Arrhenius plot (Fig. 4) yields thermal activation energy according to $I\alpha \exp(-\frac{E_A}{kT})$. The estimated thermal activation energy of 270 meV, which is much smaller in value compared with band gap of GaN (3.4 eV at room temperature) and is attributed to the thermal excitation of electrons from deep trap state or trap state near the metal-semiconductor interface into a continuum of states associated with each conductive dislocation [20]. Miller et al. associated this thermally activated process to trap assisted tunneling [10].

The decrease in the estimated thermal activation energy of an electron from trap state decreased with an increasing electric field (Fig. 5), and is attributed to the lowering of the Columbic potential barrier [19] due to the electric field. Fig. 5, a plot of E_A versus square root of electric field suggests Poole-Frenkel emission or field assisted thermal ionization to be the reverse leakage current mechanism. The relation between activation energy and electric field is [23]

$$E_A = \varphi_{PF} - \beta_{PF} E^{1/2} \tag{4}$$

here φ_{PF} is emission barrier height for carriers trapped in deep levels, β_{PF} is PF coefficient and E is applied electric field, which can obtained from the expression, $E = \sqrt{\frac{2qN_D}{\varepsilon_s}\left(V + V_{bi} - \frac{k_B T}{q}\right)}$ by substituting obtained values of built-in potential (V_{bi}) and donor density (N_d), which are obtained from the C-V characteristics.

Fig. 5 shows the plot of estimated activation energies (E_a) in the temperature range 260–420 K as a function of square root of electric field (E_r) for Au/Ni/GaN SBD. The values of an emission barrier height (φ_t) and PF coefficient (β_{PF}) obtained for GaN from intercept and slope of the linear fit for E_a versus $E_r^{1/2}$ plot are 0.63 eV and 7.31×10^{-4} eVV$^{-1/2}$cm$^{1/2}$ respectively, well consistent with reported values [23]. Thus the PF emission model in explaining the reverse current transport mechanism associated with thermally activated current component with trap assisted tunneling process.

Thus, the mechanism of reverse bias leakage current flow at low temperature is mainly due to electrons hopping from one deep trap to another deep trap [20]. Several studies have shown that the deep level defects in GaN using deep level transient spectroscopy (DLTS) technique, with activation energies 0.18–0.27 eV, 0.49 eV, 0.58 eV, 0.67 eV and 0.97 eV below the

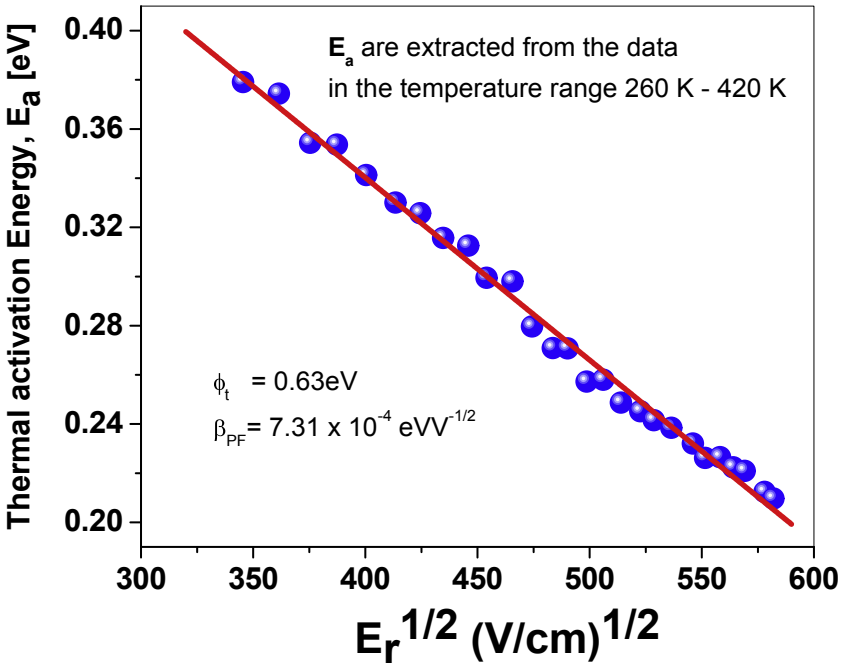

Fig. 5. The plot of thermal activation energies extracted from Arrhenius plot at different biases above 260 K versus electric field in the depletion region for Au/Ni/GaN SBD.

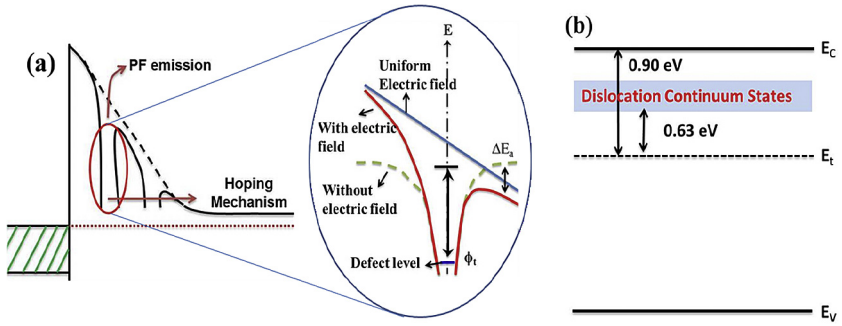

Fig. 6. (a) Schematic diagram of Poole-Frenkel emission hopping conduction of an electron in metal/semiconductor structure under reverse bias and the inset shows the schematic of the Poole-Frenkel effect. (b) A Schematic energy band diagram showing postulated trap state and dislocation continuum of states with respect to conduction band in GaN.

conduction band [24–27]. At high temperature (>260 K), the process that governs leakage current by thermal activation of electrons from deep centers can be enhanced by electric field [28].

Fig. 6(a) shows the schematic diagram of electron emission from a deep trap by Poole-Frenkel effect at high temperature and hopping conduction at low temperature. The thermally activated electrons from a deep trap states into a continuum of states associated with conductive threading dislocation enabling the reverse leakage current [Fig. 6(b)]. Hence, our experimental results showed the emission barrier height (φ_t) is 0.63 eV, which is in good agreement with the reported value 0.65 eV [14] by Ha et al. Thus, we suggest that there two main conduction processes are VRH and PF emission at low and high temperatures respectively, govern excess reverse bias leakage current via continuum of the states associated with a conductive dislocation states.

4. Conclusions

In summary, temperature-dependent reverse bias I-V characteristics in the rage of 140 and 420 K in steps of 10 K is used to evaluate possible physical mechanisms of reverse leakage current transport for Au/Ni/GaN Schottky barrier diode. Our findings present that, the variation of carrier concentration over the small depletion width obtained from the room temperature capacitance-voltage (C-V) indicates a strong internal electric field presence in the depletion region. A reduction in

barrier height with increasing reverse bias is observed. A detailed analysis of I-V characteristics suggested two mechanisms VRH and PF emission conductions in low and high temperatures respectively under the reverse bias for Au/Ni/GaN SBD.

Acknowledgement

This work is supported by University of Delhi RC/2014/6820, R & D Project and the Ministry of Trade, Industry & Energy (MOTIE, Korea) under Industrial Technology Innovation Program No.10062221, 'Development of large scale GaN epitaxy wafer for 600 V high voltage operation'.

References

[1] Robert F. Service, Science 327 (2010) 1598.
[2] H. Onodera, K. Horio, Semicond. Sci. Technol. 27 (2012), 085016.
[3] Z.Z. Bandic, P.M. Bridger, E.C. Piquette, T.C. McGill, R.P. Vaudo, V.M. Phanse, J.M. Redwing, Appl. Phys. Lett. 74 (1999) 1266.
[4] Y.-K. Kuo, T.-H. Wang, J.-Y. Chang, M.-C. Tsai, Appl. Phys. Lett. 99 (2011), 091107.
[5] Valentin O. Turin, Alexander A. Balandin, J. Appl. Phys. 100 (2006), 054501.
[6] J. Elsner, R. Jones, P.K. Sitch, V.D. Porezag, M. Elstner, Th Frauenheim, M.I. Heggie, S. Oberg, P.R. Briddon, Phys. Rev. Lett. 79 (1997) 3672.
[7] E.J. Miller, D.M. Schadt, E.T. Yu, P. Waltereit, C. Poblenz, J.S. Speck, Appl. Phys. Lett. 82 (2003) 1293.
[8] N. Miura, T. Nanjo, M. Suita, T. Oishi, Y. Abe, T. Ozeki, H. Ishikawa, T. Egawa, T. Jimbo, Solid-Sate Electron. 48 (5) (2004) 689.
[9] H. Hasegawa, S. Oyama, J. Vac. Sci. Technol. B 20 (4) (2002) 1647.
[10] E.J. Miller, E.T. Yu, P. Waltereit, J.S. Speck, Appl. Phys. Lett. 84 (2004) 535.
[11] P. Pipinys, V. Lapeika, J. Appl. Phys. 99 (2006), 093709.
[12] H. Zhang, E.J. Miller, E.T. Yu, J. Appl. Phys. 99 (2006), 023703.
[13] P.K. Rao, B. Park, S.-T. Lee, Y.-K. Noh, M.-D. Kim, J.-E. Oh, J. Appl. Phys. 110 (2011), 013716.
[14] W.J. Ha, S. Chhajed, S.J. Oh, S. Hwang, J.K. Kim, J.H. Lee, K.S. Kim, Appl. Phys. Lett. 100 (2012), 132104.
[15] D.K. Schroder, Semiconductor Materials and Devices Characterization, second ed., John Wiley & Sons, Inc., Hoboken, 1998.
[16] S.M. Sze, K.K. Ng, Physics of Semiconductor Devices, third ed., John Wiley & Sons, Inc., Hoboken, 2007.
[17] N. Yıldırım, K. Ejderha, A. Turut, J. Appl. Phys. 108 (2010), 114506.
[18] M. Musolino, D. van Treeck, A. Tahraoui, L. Scarparo, C. De Santi, M. Meneghini, E. Zanoni, L. Geelhaar, H. Riechert, J. Appl. Phys. 119 (2016), 044502.
[19] Q. Shan, David Meyaard, Q. Dai, J. Ch, E. Fred Schubert, J. Kon Son, C. Sone, Appl. Phys. Lett. 99 (2011), 253506.
[20] D. Tomer, S. Rajput, L.J. Hudy, C.H. Li, L. Li, Appl. Phys. Lett. 106 (2015), 173510.
[21] D. Emin, Phys. Rev. Lett. 32 (1974) 303.
[22] D.C. Look, D.C. Reynolds, W. Kim, O. Aktas, A. Botchkarev, V. Salvador, H. Morkoc, J. Appl. Phys. 80 (5) (1996) 2960.
[23] S. Jeong, H. Kim, J. Vac. Sci. Technol. B 33 (2) (2015), 021205–1.
[24] C.D. Wang, L.S. Yu, S.S. Lau, E.T. Yu, W. Kim, A.E. Botchkarev, H. Morkoc, Appl. Phys. Lett. 72 (1998) 1211.
[25] F.D. Auret, S.A. Goodman, F.K. Koschick, J.-M. Spaeth, B. Beaumont, P. Gibart, Appl. Phys. Lett. 73 (1998) 3745.
[26] C.B. Soh, S.J. Chua, P. Chen, W. Liu, H. Hartono, Thin Slid Films 515 (2007) 4509–4513.
[27] C.B. Soh, S.J. Chua, F. Lim, D.Z. Chi, S. Tripathy, W. Liu, J. Appl. Phys. 96 (3) (2004) 1341.
[28] H. Zhang, E.J. Miller, E.T. Yu, J. Appl. Phys. 99 (2006), 023703.